Photocatalysts

Deutsche Ausgabe: DOI: 10.1002/ange.201509701
Internationale Ausgabe: DOI: 10.1002/anie.201509701

Modulated Binary–Ternary Dual Semiconductor Heterostructures

*Gyanaranjan Prusty, Amit K. Guria, Indranil Mondal, Anirban Dutta, Ujjwal Pal, and Narayan Pradhan**

Abstract: *A generic modular synthetic strategy for the fabrication of a series of binary-ternary group II-VI and group I-III-VI coupled semiconductor nano-heterostructures is reported. Using Ag_2Se nanocrystals first as a catalyst and then as sacrificial seeds, four dual semiconductor heterostructures were designed with similar shapes: $CdSe\text{-}AgInSe_2$, $CdSe\text{-}AgGaSe_2$, $ZnSe\text{-}AgInSe_2$, and $ZnSe\text{-}AgGaSe_2$. Among these, dispersive type-II heterostructures are further explored for photocatalytic hydrogen evolution from water and these are observed to be superior catalysts than the binary or ternary semi-conductors. Details of the chemistry of this modular synthesis have been studied and the photophysical processes involved in catalysis are investigated.*

For conversion of solar to chemical energy, semiconductor nanostructures with tunable absorption and high excitonic coefficients are being extensively studied as photocatalysts.[1] The major challenge with these nanostructures is suppressing the fast recombination of their photogenerated charge carriers. As a result, tremendous efforts have been put forward for designing ideal semiconductor nanostructures that can effectively suppress the recombination and efficiently separate the charge carriers.[1g,l,2] Notable examples include the coupling to another semiconductor or metal where the excited electron or the hole can promptly move from one material to the other.[1j,2b,f,3] Beyond the main group (for example, II-VI and III-V) leading semiconductors, different modulated heterostructures of semiconductor–semiconductor, semiconductor–metal, and dual semiconductor–metal-coupled structures, including multinary nanostructures, have been developed and explored as photocatalysts.[2d,3d,e,k,4] One ideal case are the type-II semiconductor heterostructures, which can efficiently separate the charge carriers.[2b,5] However, as catalysis is a surface phenomenon, appropriate semiconductor materials and shape architectures are essential for transportation of these carriers to the redox species. Thus, well-planned modular synthetic strategies are necessary for designing such structures with multiple semiconductors.

Herein, we report a generic modulated synthetic strategy with a dual-mode growth mechanism for coupling group II-VI and I-III-VI semiconductor nanostructures. Using Ag_2Se as a sacrificial seed, and employing the superionic conductor catalytic as well as diffusion control growths, four binary–ternary heterostructures, $CdSe\text{-}AgInSe_2$, $CdSe\text{-}AgGaSe_2$, $ZnSe\text{-}AgInSe_2$, and $ZnSe\text{-}AgGaSe_2$, were designed without common cations. Three of these heterostructures follow type-II combinations, and one follows type-I. Further, appropriate type-II nanostructures were explored for catalytic hydrogen evolution from water. On comparison, type-II dual semiconductors were observed as more efficient catalysts than the binary or ternary nanostructures. The formation chemistry, characterization, and photorecombination of these coupled heteronanostructures have been thoroughly investigated.

Synthetic procedures for the fabrication of such modulated nanostructures are shown schematically in Figure 1 a–c. This is a combination of two-step growth processes; one is the superionic conductor catalytic growth, and other is diffusion controlled growth. Figure 1 a shows the catalytic growth using Ag_2Se as superionic conductor catalyst,[6] where $Ag_2Se\text{-}M^{II}Se$ ($M^{II} = Cd^{2+}$, Zn^{2+}) remains the ultimate products. Here, the catalyst Ag_2Se retains its shape, size, and crystal structure. The synthetic procedure for diffusion-controlled growth using Ag_2Se seeds in presence of M^{III} (In^{III}, Ga^{III}) precursors leading to $AgM^{III}Se_2$ nanostructures[7] is shown in Figure 1 b. In this process, Ag_2Se is sacrificed during the course of formation of tadpole-like $AgM^{III}Se_2$ nanostructures. The combination of both these processes is further depicted in Figure 1 c, where $M^{II}Se\text{-}AgM^{III}Se_2$ heterostructures are the resulting products.

In a typical synthesis, seed Ag_2Se nanocrystals were synthesized following selenization of Ag(0) in oleylamine using elemental Se as the selenium source. For superionic conductor catalytic growth of CdSe, cadmium–acetate was introduced at 130 °C, and for ZnSe growth, zinc–acetate was injected at 180 °C. The reaction temperature was then increased to 230 °C for Ga^{III} or In^{III} precursor (respective acetylacetonates) injection, and annealed at 250 °C for the formation of the binary–ternary heterostructures. Details of the synthesis have been provided in the Supporting Information.

Figure 1 d–g shows representative TEM images of $CdSe\text{-}AgGaSe_2$, $CdSe\text{-}AgInSe_2$, $ZnSe\text{-}AgGaSe_2$, and $ZnSe\text{-}AgInSe_2$ coupled structures with nearly identical shapes. To our knowledge, these are the first example of group II-VI and I-III-VI coupled semiconductor heterostructures. The High Angle Annular Dark Field (HAADF) images of $ZnSe\text{-}AgGaSe_2$ and $CdSe\text{-}AgGaSe_2$ heterostructures are shown in Figure 1 h and 1 i, respectively, and from the elemental mapping data, it was confirmed that the head parts are group I-III-VI and tail parts are group II-VI semiconductors.

---

[*] G. Prusty, A. K. Guria, A. Dutta, Dr. N. Pradhan
Department of Materials Science and Centre for Advanced Materials
Indian Association for the Cultivation of Science
Kolkata 700032 (India)
http://iacs.res.in/matsc/msnp/
E-mail: camnp@iacs.res.in

I. Mondal, Dr. U. Pal
Chemistry and Biomimetics Group
CSIR-Central Mechanical Engineering Research Institute
M.G Avenue, Durgapur-713209 (India)

Supporting information for this article is available on the WWW under http://dx.doi.org/10.1002/anie.201509701.

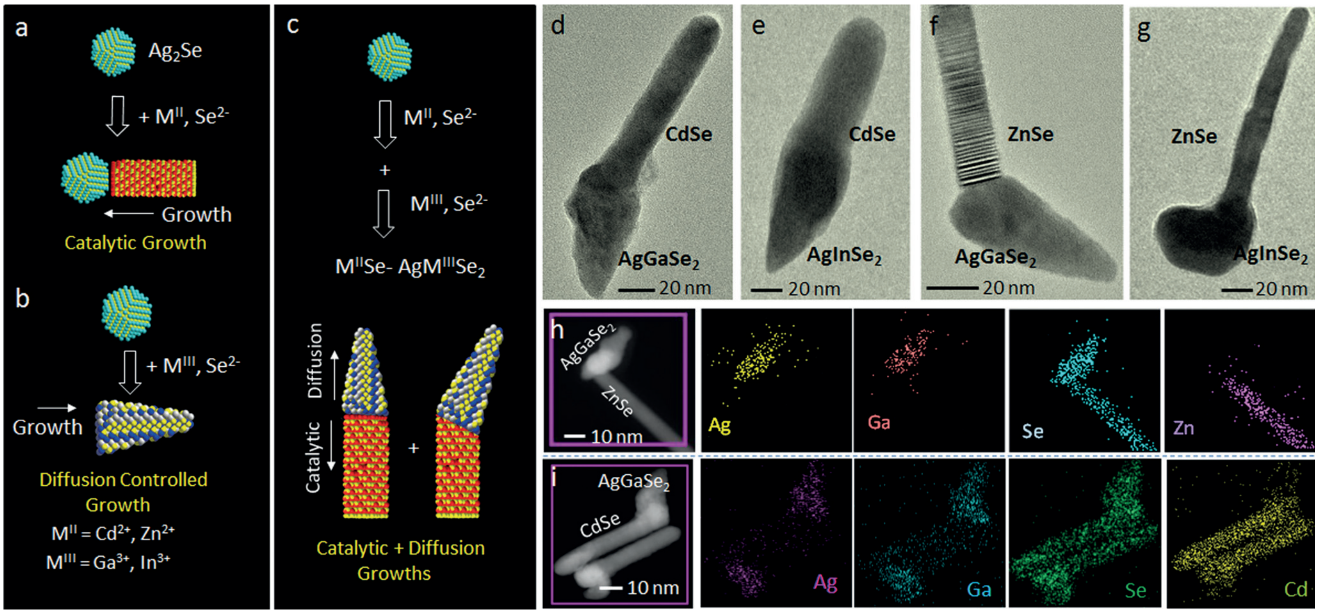

Figure 1. a–c) The modular synthesis schemes for architecting binary-ternary dual semiconductor nanostructures. a) Superionic conductor catalytic growth using Ag_2Se seeds and resulting binary-binary heterostructures where Ag_2Se seeds remain intact. b) Diffusion-controlled growth forming ternary tadpole structures where the seed Ag_2Se is sacrificed. c) Combined catalytic and diffusion growth leading to a series of binary–ternary heterostructures. d–g) Representative TEM images for CdSe-$AgGaSe_2$, CdSe-$AgInSe_2$, ZnSe-$AgGaSe_2$, and ZnSe-$AgInSe_2$, respectively. h) HAADF-STEM image of a single heterostructure of ZnSe-$AgGaSe_2$ and the elemental mapping for elements Ag, Ga, Se, and Zn. i) HAADF-STEM image of a pair of CdSe-$AgGaSe_2$ heterostructures and the elemental mapping of elements Ag, Ga, Se, and Cd.

The length of each part of the heterostructures varies from one to other, depending on the reactivity of the precursors used and also on the reaction condition. As the growth of ZnSe is faster than CdSe on Ag_2Se, ZnSe has larger binary semiconductor lengths and also remains broadly dispersed. However, for CdSe-$AgM^{III}Se_2$, the length of CdSe remains smaller and their size remains nearly monodispersed (Supporting Information).

To support our adopted mechanism, we have also analyzed the products in controlled reactions and in the intermediate stages. TEM images of seed Ag_2Se nanocrystals and the obtained tadpole-shaped $AgGaSe_2$ and $AgInSe_2$ nanostructures on treatment with Ga^{III} and In^{III} ions, respectively, are shown in Figure 2a–c respectively. A typical shape of the catalytically grown CdSe-Ag_2Se binary–binary intermediate heterostructure, obtained from Ag_2Se as the first product, is also shown in Figure 2d (also see the Supporting Information, Figure S1). For the case of ZnSe-Ag_2Se, similar intermediate heterostructures were also obtained.[6] Wide-view TEM images of CdSe-$AgInSe_2$, CdSe-$AgGaSe_2$, ZnSe-$AgInSe_2$, and ZnSe-$AgGaSe_2$ obtained with our adopted two-step procedure are shown in Figure 2e–h. More TEM images are provided in the Supporting Information (Figure S2–4). High-resolution TEM (HRTEM) images showing the heterojunctions for all coupled II-VI and I-III-VI semiconductors were also obtained and analyzed (Figure S5–7)

Powder X-ray diffractions of all four heterostructures were carried out to investigate the phase of the semiconductor heterostructures (Figure S8). From the peak positions, it was revealed that CdSe and ZnSe are in wurtzite (WZ) and zinc blende (ZB) phases, respectively, though in both cases some percentage of mixed phases were also obtained. Similar mixed phase are also reported in literature.[6] $AgInSe_2$ was obtained in orthorhombic (Ortho) and $AgGaSe_2$ in tetragonal (Tg) phase in both the CdSe- as well as ZnSe-coupled cases. HRTEM analysis suggests the coupling directions for CdSe-$AgInSe_2$, CdSe-$AgGaSe_2$, ZnSe-$AgGaSe_2$, and ZnSe-$AgInSe_2$ coupled structures to be along [010]-[120], [100]-[112], [111]-[112], and [111]-[120] respectively. EDS spectra for each set of coupled structures are shown in the Supporting Information (Figure S9).

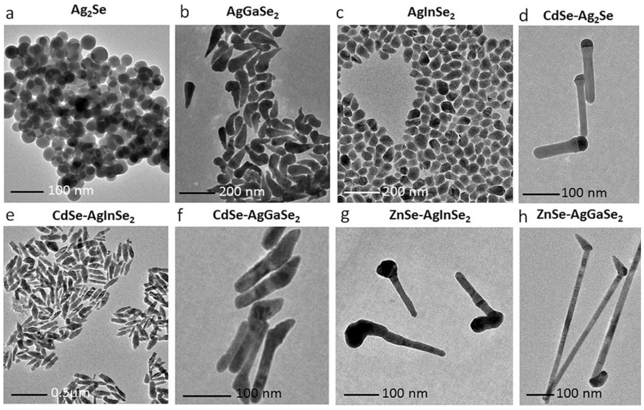

Figure 2. TEM image of a) seed Ag_2Se nanocrystals; b) $AgGaSe_2$ tadpoles; c) $AgInSe_2$ tadpoles obtained under controlled reactions; d) intermediate CdSe-Ag_2Se; and dual semiconductors e) CdSe-$AgInSe_2$, f) CdSe-$AgGaSe_2$, g) ZnSe-$AgInSe_2$, and h) ZnSe-$AgGaSe_2$.

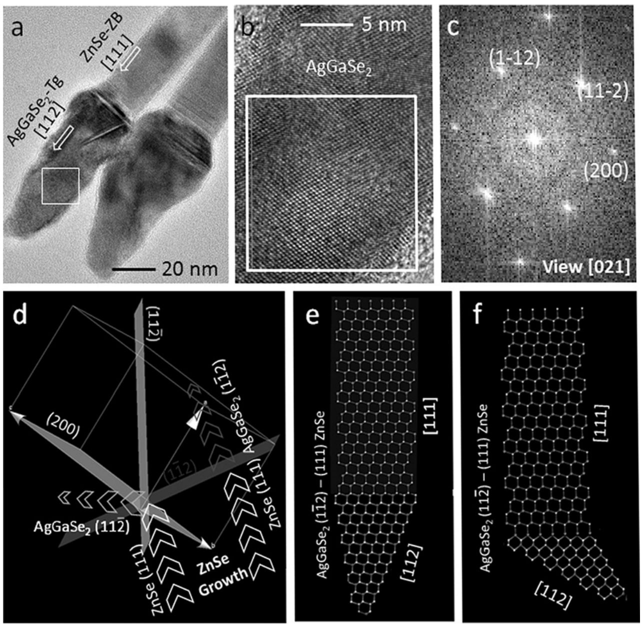

Figure 3. a) TEM image showing coupled structures of ZnSe and $AgGaSe_2$. b) HRTEM of $AgGaSe_2$ head. c) Selected area FFT pattern from the $AgGaSe_2$ part of the heterostructure. d) Possible growth directions of $AgGaSe_2$ on ZnSe during diffusion of Ag into gallium–selenide. Arrow mark shows ZnSe growth direction. e, f) Atomic models of the heterostructures of ZnSe-$AgGaSe_2$ showing the growth of tadpole heads along linear and 120 degree angle with ZnSe.

Interestingly, in most of the cases, the ternary tadpole is either connected linearly or at an angle of ≈ 120 degrees with binary CdSe or ZnSe nanostructures (Figure 1 c). This was analyzed in detail for ZnSe-$AgGaSe_2$ (Figure 3). Figure 3 a presents a typical HRTEM showing linearly grown tadpole on binary ZnSe. Figure 3 b and c present the HRTEM of the tadpole part and selected area FFT pattern. The analysis suggests that tadpole growth through diffusion could be possible along either of two identical group of directions on binary ZnSe nanostructures, as shown in Figure 3 d. Here, the tadpole $AgGaSe_2$ can grow either along [1-12] or [11-2] directions, making a line or at an angle of 120 degree with ZnSe. Atomic models showing the possible patterns of growth are further presented in Figure 3 e, f.

The UV-visible spectra of all of the heterostructures were measured for their possible harvesting of solar light, and it was observed that all of them absorb in the visible spectral window (Figure S10). However, as the length of ZnSe remains more because of their faster growth, the dispersity of these structures is poor. As a result, we chose the CdSe-based heterostructures for studying solar light harvesting for photocatalytic hydrogen evolution from water.

Figure 4 a and b show the amount of hydrogen evolution with time for CdSe-$AgInSe_2$ and CdSe-$AgGaSe_2$ dual semiconductors respectively. For the control reaction, the catalytic activities are also studied for CdSe nanorods,[8] $AgInSe_2$, and $AgGaSe_2$[9a] tadpoles prepared separately. TEM images of $AgGaSe_2$ and $AgInSe_2$ used for the control reactions are shown in Figure 2 b and c, respectively. Interestingly, while compared with CdSe and $AgInSe_2$ individually, their coupled structures showed multifold enhancements of hydrogen evolution under identical conditions (from 100–200 to 1600 $\mu mol\,g\,m^{-1}$). Similarly, the heterostructures of CdSe-$AgGaSe_2$ performed better in comparison to their individual counterpart. Here, we have studied the catalytic activity following standard procedures.[3e] Details of the experiment are provided in the Supporting Information. For stability and reproducibility, multiple cycles of irradiation of the catalysts were carried out, and all of them were found to be stable for more than 24 h. A typical recycling measurement is shown in Figure 4 c, which demonstrates the reproducibility. A histogram of hydrogen evolution for each of the different catalysts is shown in Figure 4 d for comparison. These results indicate that the heterostructures are superior catalysts for conversion of light to chemical energy and evolution of hydrogen from water.

To understand the enhanced catalytic activities of these binary–ternary heterostructures, the bandgap alignments of all these semiconductors were analyzed. Figure S11a depicts the bulk valence and conduction bands of all of the involved semiconductors, and the positions suggest that CdSe-$AgGaSe_2$ and ZnSe-$AgGaSe_2$ form typical type-II structure, and CdSe-$AgInSe_2$ forms a pseudo-type-II, but ZnSe-

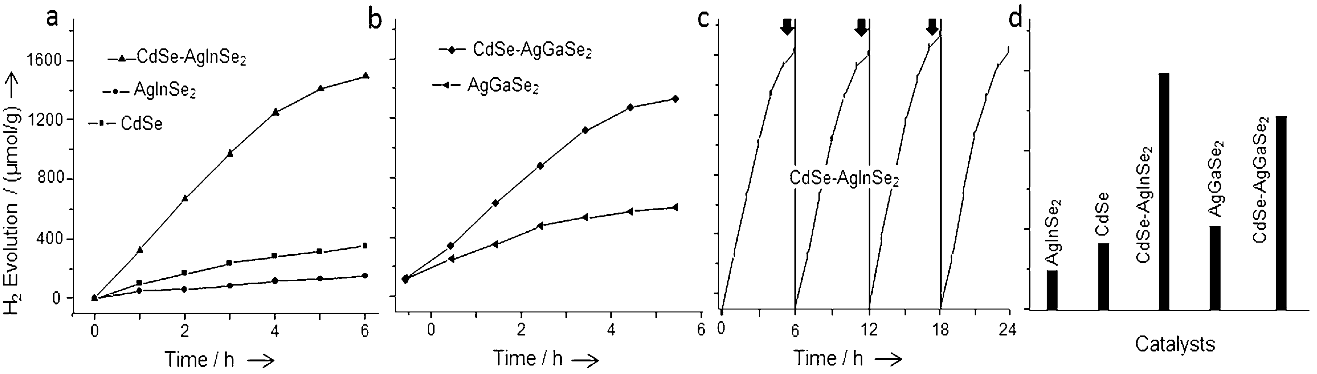

Figure 4. a, b) Hydrogen evolution plots using CdSe-$AgInSe_2$ and CdSe-$AgGaSe_2$ dual semiconductor heterostructures, respectively. c) Cycling hydrogen generation. Arrows indicate the evacuations. d) Histograms showing the relative amount of hydrogen evolution using different catalysts, obtained after six hours of reaction.

AgInSe$_2$ forms a type-I structure. Restricting the discussions with CdSe, it can be presumed here that the pseudo-type-II alignments of CdSe-AgInSe$_2$, where the excited photoelectron in the valence band tunnels for a longer time because of the similar energy of both semiconductors, resulting in the maximum possibility for transfer to water for triggering reduction of H$^+$ to H$_2$. For the case of CdSe-AgGaSe$_2$, the excited electron from CdSe moved to AgGaSe$_2$ and mostly resides on its conduction band. This provides more opportunities for it to transfer to water and trigger the reduction. Such carrier transfer is not possible for single semiconductors, such as CdSe and AgIn(or Ga)Se$_2$, and thus they showed lower photocatalytic activity. Possible modes of electron and hole transfer in these two heterostructures are shown in Figure S11 b–c, where the predominant excitation from CdSe nanostructures has been assumed because of their higher absorption coefficient than the ternary semiconductor.

In conclusion, a modular synthetic procedure for fabricating group II-VI and I-III-VI binary–ternary dual semiconductor heterostructures is reported. Among these, type-II heterostructures involving CdSe were explored for photocatalytic evolution of hydrogen from water, and observed to be superior catalysts in comparison to the individual binary or ternary semiconductors. The synthetic approach with coupling of two different groups of semiconductors and their efficient catalytic activities provides new insights for developing functional materials, and also encourages their implementations in different fields.

Acknowledgements

DST of India (SR/ST/IC-68/2010, SJF/CSA-01/2010-11) is acknowledged for funding.

Keywords: binary–ternary · heterostructures · photocatalyst · tadpoles

How to cite: *Angew. Chem. Int. Ed.* **2016**, *55*, 2705–2708
Angew. Chem. **2016**, *128*, 2755–2758

[1] a) P. V. Kamat, *Chem. Rev.* **1993**, *93*, 267; b) X. Chen, S. Shen, L. Guo, S. S. Mao, *Chem. Rev.* **2010**, *110*, 6503; c) M. G. Walter, E. L. Warren, J. R. McKone, S. W. Boettcher, Q. Mi, E. A. Santori, N. S. Lewis, *Chem. Rev.* **2010**, *110*, 6446; d) M. D. Kärkäs, O. Verho, E. V. Johnston, B. Aakermark, *Chem. Rev.* **2014**, *114*, 11863; e) J. Chen, X.-J. Wu, L. Yin, B. Li, X. Hong, Z. Fan, B. Chen, C. Xue, H. Zhang, *Angew. Chem. Int. Ed.* **2015**, *54*, 1210; *Angew. Chem.* **2015**, *127*, 1226; f) K. Li, R. Chen, S.-L. Li, M. Han, S.-L. Xie, J.-C. Bao, Z.-H. Dai, Y.-Q. Lan, *Chem. Sci.* **2015**, *6*, 5263; g) V. L. Bridewell, R. Alam, C. J. Karwacki, P. V. Kamat, *Chem. Mater.* **2015**, *27*, 5064; h) T. Kato, Y. Hakari, S. Ikeda, Q. Jia, A. Iwase, A. Kudo, *J. Phys. Chem. Lett.* **2015**, *6*, 1042; i) F. Wen, C. Li, *Acc. Chem. Res.* **2013**, *46*, 2355; j) H. Song, *Acc. Chem. Res.* **2015**, *48*, 491; k) W. Wang, J. Chen, C. Li, W. Tian, *Nat. Commun.* **2014**, *5*, 4647; l) Z. Sun, Q. Yue, J. Li, J. Xu, H. Zheng, P. Du, *J. Mater. Chem. A* **2015**, *3*, 10243; m) E. Khon, K. Lambright, R. S. Khnayzer, P. Moroz, D. Perera, E. Butaeva, S. Lambright, F. N. Castellano, M. Zamkov, *Nano Lett.* **2013**, *13*, 2016.

[2] a) J. S. DuChene, B. C. Sweeny, A. C. Johnston-Peck, D. Su, E. A. Stach, W. D. Wei, *Angew. Chem. Int. Ed.* **2014**, *53*, 7887; *Angew. Chem.* **2014**, *126*, 8021; b) C. Eley, T. Li, F. Liao, S. M. Fairclough, J. M. Smith, G. Smith, S. C. E. Tsang, *Angew. Chem. Int. Ed.* **2014**, *53*, 7838; *Angew. Chem.* **2014**, *126*, 7972; c) Q. Li, B. Guo, J. Yu, J. Ran, B. Zhang, H. Yan, J. R. Gong, *J. Am. Chem. Soc.* **2011**, *133*, 10878; d) I. Tsuji, H. Kato, H. Kobayashi, A. Kudo, *J. Am. Chem. Soc.* **2004**, *126*, 13406; e) R. Costi, A. E. Saunders, E. Elmalem, A. Salant, U. Banin, *Nano Lett.* **2008**, *8*, 637; f) U. Banin, Y. Ben-Shahar, K. Vinokurov, *Chem. Mater.* **2014**, *26*, 97; g) C. Harris, P. V. Kamat, *ACS Nano* **2009**, *3*, 682.

[3] a) S. Cao, Y. Chen, C.-J. Wang, X.-J. Lv, W.-F. Fu, *Chem. Commun.* **2015**, *51*, 8708; b) R. Costi, A. E. Saunders, U. Banin, *Angew. Chem. Int. Ed.* **2010**, *49*, 4878; *Angew. Chem.* **2010**, *122*, 4996; c) R. Bose, A. H. M. Abdul Wasey, G. P. Das, N. Pradhan, *J. Phys. Chem. Lett.* **2014**, *5*, 1892; d) L. Amirav, A. P. Alivisatos, *J. Phys. Chem. Lett.* **2010**, *1*, 1051; e) X. Yu, A. Shavel, X. An, Z. Luo, M. Ibáñez, A. Cabot, *J. Am. Chem. Soc.* **2014**, *136*, 9236; f) X. Yu, J. Liu, A. Genc, M. Ibanez, Z. Luo, A. Shavel, J. Arbiol, G. Zhang, Y. Zhang, A. Cabot, *Langmuir* **2015**, *31*, 10555; g) X. Yu, X. An, A. Genc, M. Ibanez, J. Arbiol, Y. Zhang, A. Cabot, *J. Phys. Chem. C* **2015**, *119*, 21882; h) P. D. Cozzoli, T. Pellegrino, L. Manna, *Chem. Soc. Rev.* **2006**, *35*, 1195; i) M. Okano, M. Sakamoto, T. Teranishi, Y. Kanemitsu, *J. Phys. Chem. Lett.* **2014**, *5*, 2951; j) K. Wu, W. E. Rodríguez-Córdoba, Y. Yang, T. Lian, *Nano Lett.* **2013**, *13*, 5255; k) S. Deka, A. Falqui, G. Bertoni, C. Sangregorio, G. Poneti, G. Morello, M. De Giorgi, C. Giannini, R. Cingolani, L. Manna, P. D. Cozzoli, *J. Am. Chem. Soc.* **2009**, *131*, 12817; l) G. Manna, R. Bose, N. Pradhan, *Angew. Chem. Int. Ed.* **2014**, *53*, 6743; *Angew. Chem.* **2014**, *126*, 6861; m) Z. W. Seh, S. Liu, M. Low, S.-Y. Zhang, Z. Liu, A. Mlayah, M.-Y. Han, *Adv. Mater.* **2012**, *24*, 2310.

[4] a) T.-T. Zhuang, Y. Liu, M. Sun, S.-L. Jiang, M.-W. Zhang, X.-C. Wang, Q. Zhang, J. Jiang, S.-H. Yu, *Angew. Chem. Int. Ed.* **2015**, *54*, 11292; *Angew. Chem.* **2015**, *127*, 11446; b) L. Amirav, F. Oba, S. Aloni, A. P. Alivisatos, *Angew. Chem. Int. Ed.* **2015**, *54*, 7007; *Angew. Chem.* **2015**, *127*, 7113.

[5] a) Y. Wang, Q. Wang, X. Zhan, F. Wang, M. Safdar, J. He, *Nanoscale* **2013**, *5*, 8326; b) S. Kim, B. Fisher, H.-J. Eisler, M. Bawendi, *J. Am. Chem. Soc.* **2003**, *125*, 11466; c) B. Blackman, D. Battaglia, X. Peng, *Chem. Mater.* **2008**, *20*, 4847.

[6] A. K. Guria, S. Sarkar, B. K. Patra, N. Pradhan, *J. Phys. Chem. Lett.* **2014**, *5*, 732.

[7] a) J. Wang, K. Chen, M. Gong, B. Xu, Q. Yang, *Nano Lett.* **2013**, *13*, 3996; b) J. Zhou, F. Huang, J. Xu, Y. Wang, *Nanoscale* **2013**, *5*, 9714.

[8] A. Figuerola, M. van Huis, M. Zanella, A. Genovese, S. Marras, A. Falqui, H. W. Zandbergen, R. Cingolani, L. Manna, *Nano Lett.* **2010**, *10*, 3028.

[9] a) G. Prusty, A. K. Guria, B. K. Patra, N. Pradhan, *J. Phys. Chem. Lett.* **2015**, *6*, 2421; b) T. Bai, C. Li, F. Li, L. Zhao, Z. Wang, H. Huang, C. Chen, Y. Han, Z. Shi, Z. S. Fenga, *Nanoscale* **2014**, *6*, 6782.

Received: October 16, 2015
Revised: December 21, 2015